J Mol Model (2010) 16:1651–1670
DOI 10.1007/s00894-010-0670-3

ORIGINAL PAPER

In silico point mutation and evolutionary trace analysis applied to nicotinic acetylcholine receptors in deciphering ligand-binding surfaces

Marimuthu Parthiban · Piramanayagam Shanmughavel · Ramanathan Sowdhamini

Received: 17 June 2009 / Accepted: 13 December 2009 / Published online: 5 March 2010

Abstract The nicotinic acetylcholine receptors (nAChRs) are members of the Cys-loop superfamily and contain ligand gated ion channels (LGIC). These receptors are located mostly in the central nervous system (CNS) and peripheral nervous system (PNS). nAChRs reside at pre-synaptic regions to mediate acetylcholine neurotransmission and in the post synaptic membrane to propagate nerve impulses through neurons via acetylcholine. Malfunction of this neurotransmitter receptor is believed to cause various neurodegenerative diseases, such as Alzheimer's disease, Parkinson's disease and schizophrenia, and nAChRs are thus important drug targets. In the present work, starting from an earlier model of pentameric α_7nAChR, a considerable effort has been taken to investigate interaction with ligands by performing docking studies with a diverse array of agonists and antagonists. Analysis of these docking complexes reveals identification of possible ligand-interacting residues. Some of these residues, e.g. Ser34, Gln55, Ser146, and Tyr166, which are evolutionarily conserved, were specifically subjected to virtual mutations based on their amino acid properties and found to be highly sensitive in the presence of antagonists by docking. Further, the study was extended using evolutionary trace analysis, revealing conserved and class-specific residues close to the putative ligand-binding site, further supporting the results of docking experiments.

Keywords nAChR · Molecular docking · Evolutionary trace analysis · In silico point mutation · Ligand binding domain · Neurodegenerative disease

M. Parthiban · P. Shanmughavel
Department of Bioinformatics, Bioinformatics Centre and Computational Biology Laboratory, Bharathiar University, Coimbatore 641064, India

M. Parthiban · R. Sowdhamini (✉)
Tata Institute of Fundamental Research, National Centre for Biological Sciences, GKVK-UAS campus Bellary road, Bangalore 560065, India
e-mail: mini@ncbs.res.in

Introduction

More than one-half of current drugs target membrane proteins. A significant proportion of these membrane proteins are involved in diverse functions like signal transduction. Nicotinic acetylcholine receptors (nAChRs)—integral membrane proteins with cationic channels that express an excitatory response both in neurons and muscles—are one such class of membrane protein receptors [1]. nAChRs were the first ion channel and membrane receptor of a neurotransmitter to be isolated (chemically identified by Salvaterra and Moore in 1973 [2]), and remain one of the best known membrane proteins involved in signal transduction.

nAChRs mediate synaptic transmission in many parts of the central nervous systems (CNS) and peripheral nervous systems (PNS) in vertebrates. nAChRs play a vital role in perception, cognition, emotion and pain, and are also equally involved in signal transduction in the autonomic ganglia, retina and adrenal medulla. They are located on the surfaces of cytoplasmic membranes in the CNS and PNS. Channel opening is induced by neurotransmitters like acetylcholine (ACh) or nicotine. Neurotransmitter binding results in depolarization of the membrane, leading to modulation of either neuronal activity or muscle contraction. These receptors have been implicated in diverse functions

such as stabilizing synapse formation during development, learning and memory, and neuronal survival [3].

The recent determination of the crystal structure of the acetylcholine binding protein (AChBP) of the great pond snail (*Lymnaea stagnalis*) has been an important milestone in this area. The subunit shares sequence similarity of about 22–27% with the N-terminal extracellular domain (ECD) of nAChR and related channels and has all the structural hallmarks of α7 ECDs [4]. Thus, AChBP can be used as a structural template for modeling the ECD of nAChR and related channels [5]. Apart from the structural similarity of AChBP in that it forms a homopentamer, it is also highly sensitive to α-bungarotoxin (α-BTX) and other α_7nAChR cholinergic ligands with comparable affinities, making it a suitable structural model for α_7nAChR [6].

Spectroscopic studies conducted on the recombinant amino-terminal ECD of various nAChR subunits revealed that the ECDs of nAChRs contain a high proportion of residues belonging to β-strands. The AChBP monomer has a short α-helix at the N-terminus, followed by two short 3_{10} helices and ten β-strands, termed β_1–β_{10}. The protein conforms to a modified immunoglobulin (Ig) topology in which an inner β-sheet (composed of β_1, β_2, β_3 β_5, β_6 and β_8) is linked to an outer β-sheet (composed of β_4, β_7, β_9 and β_{10}) by means of a "cys-loop" disulfide bridge between Cys123 and Cys136, and is organized in a curled β-sandwich. The cys-loop is a feature of the N-terminus of the ACh ion channel superfamily, and can be found between Cys126 and Cys140 of α_7nAChR. The only contacts between the subunits of the pentamer are the two dimer interfaces of each protomer. There are five nAChR ligand binding sites, located at these five protomer interfaces, close to the outside surface of the pentameric AChBP ring [7].

The residues forming the binding pockets are highly conserved between members of the ligand-gated ion channel (LGIC) superfamily, despite the poor homology of the residues lining the interface between protomer pairs. In addition, the nAChR subunit contains three potential sites of N-linked glycosylation (N22, N68 and N111) within the ECD, although the absence of glycosylation does not appear to affect ligand binding. The binding of either an agonist or antagonist to the binding pockets in the ECD may cause changes in the molecular structure of the receptor, which are then transduced to the transmembrane domain (TMD) resulting in the opening or closing of the ion channel [8].

The TMD of α_7nAChR is composed of four putative α-helices or membrane spanning region (MSR), consisting of an average of 19–24 amino acids (MSR I-24, II-19, III-20 and IV-19). There exists a short cytoplasmic region between MSR I and II [7] and a short extracellular (EC) region between MSR II and III. A large intracellular domain exists, however, between MSR III and IV [9].

Four functional states have been described in nAChRs: the resting (closed) state, the open state, the fast-onset desensitized (closed) state, and the slow-onset desensitized (closed) state. The resting state is the most stable state in the absence of agonist, and the slow-onset desensitized state is the most stable state in the presence of agonist. The open state and the fast-onset desensitized state are metastable states, in that their concentrations rise transiently and reach a very low value at equilibrium. After prolonged exposure to ACh or nicotinic drugs, the ionic response slowly and gradually decreases, leading to a state of high affinity where the ion channel is closed—a phenomenon referred to as desensitization [10].

Protein chemistry and sequence analysis studies reveal a general pattern for each polypeptide subunit of nAChR that is common for all pentameric neurotransmitter receptor channels of the Cys-loop family, including the GABA and glycine receptors. This is a well-known situation already investigated in great detail in regulatory proteins referred to as allosteric proteins. This allosteric character of nAChR is proposed to be mediated by a conformational change in the molecule. It is purported that α_7 might play a role in a range of diseases including epilepsy, schizophrenia, Alzheimer's disease and anxiety disorders [11].

The ligand binding domain (LBD) of human neuronal α_7 nAChR is a cationic channel that belongs to the LCIX superfamily, known as Cys-loop receptors. The LGIC superfamily comprises a wide variety of receptors, which includes muscle type and neuronal type nAChRs, 5-hydroxytryptamine type-3 receptors ($5HT_3$), γ-aminobutyric acid type$_A$ ($GABA_A$) and type$_C$ ($GABA_C$) receptors, Glycine receptors (GlyR), and chloride permeable glutamate receptors (GluRCl). The disulfide-linked cysteines at positions 188–189 are uniquely conserved in the α-subunit, and can be selectively labeled as the binding site [12].

There are at least 17 different nAChR subunits, which can be divided into two categories: muscle type (α_1, β_1, δ, ε, γ) and neuronal type (α_2–α_{10} and β_2–β_4). The neuronal nAChR channel is composed of five subunits, which can be subdivided into two groups: subunits carrying the principle ACh binding site component (α_2–α_{10}), and subunits carrying the complementary component of the ACh binding site (non-α or β_2–β_4). The channels formed by these subunits can be either homomeric, consisting of five subunits comprising the same type homomeric (α_7–α_9), or heteromeric, where the pentameric channel consists of two or more different subunits [13]. α_7nAChR is the only homomeric nicotinic receptors expressed in the human brain and is one of the two most abundantly expressed nicotinic receptor subtypes in the brain, the other being the heterodimer consisting of α_4 and β_2 subunits [14].

These structural data support the view that ligand binding to nAChR gives rise to a conformational transition of the receptor molecule. In this respect, nAChR appears to function as a typical allosteric protein. These basic properties are of critical importance for disease progression because mutations, which are also found in many other receptor categories, might be highly pathological. Moreover, future pharmacology of nicotinic agents (e.g., the many drugs acting on membrane receptors) should address the structural differences existing between these conformations [2].

In the present study, we use our previously generated theoretical model for docking studies with a diverse group of ligand molecules. Residues at the binding site were reported in our previous studies to be highly conserved among the superfamilies [15]. These highly conserved residues were subjected to mutagenesis and the analysis was further extended to docking studies with the same docking protocol performed in the previous step. Docked complexes were analyzed for interacting residues and the results were further substantiated by evolutionary trace analysis using their closest homologues. The ECD of neuronal type nAChR sequences of α_2, α_3, α_4, α_7 and α_9 were subjected to evolutionary trace analysis. The conserved and class-specific residues among these sequence groups, from the derived phylogenetic tree and for a particular trace alignment, were analyzed in detail for spatial distribution of polar and hydrophobic residues on the surfaces of the theoretical model. The docking of agonists versus antagonists and screening investigations for these receptors should be useful in studying the distinct and discrete (resting versus active) conformations of the protein. Such studies will make it easier for scientists to model the diversity of binding sites resulting from the diversity of subunits and to design novel leads for diverse classes of receptors.

Materials and methods

Homology model of α_7nAChR

In our previous studies, the theoretical structure of α_7nAChR was built using Modeller 9v2 [16] for all the subunits using AChBP as the template. The subunits were further assembled to form a pentamer using the SYBYL7.1 (Tripos, St.Louis, MO) package based on the initial equivalences from EBI-Dalilite [17]. The theoretical structure of the pentamer was subjected to energy minimization, using the SYBYL7.1 package, to correct the stereochemistry and the geometric inaccuracies of the theoretical model at the interface region. The energy calculations were carried out for 500 iterations using TRIPOS force field in SYBYL7.1, which did not alter the native model. For large biomolecules and multi-modular and multi-chain complexes, it is computationally time-consuming to bring the systems to convergence. The resulting model was used for further interaction studies [15].

Retrieval and processing of small molecules for interaction with α_7nAChR

Information about agonists and antagonists (Table 1) was retrieved from the PubChem database (http://pubchem.ncbi.nlm.nih.gov/). These small molecules were retrieved in standard 2D SDF format, converted into three-dimensional coordinates by applying the MMCF force field, and subsequently minimized to the standard recommended value of 50 iterations for small molecules using the VLifeMDS suite [VLifeSciences Pune, India].

Molecular docking of agonists and antagonists with α_7nAChR

The agonist and the antagonist molecules were subjected to docking with the theoretical structure of α_7nAChR using the widely used docking program AUTODOCK4 [18]. Docking was performed for all the small molecules by keeping the ligands as flexible. The grid was placed at the interface region of the theoretical model of α_7nAChR.

Table 1 List of agonist and antagonist molecules used for docking with α_7 nicotinic acetylcholine receptor (α_7nAChR). The structures were retrieved from the PubChem database (http://pubchem.ncbi.nlm.nih.gov/)

S.No	CID	Agonists
1	187	Acetylcholine
2	942	Nicotine
3	204966	Bromoacetylcholine
4	2551	Carbamylcholine
5	8425	Codeine
6	854023	Epibatidine
7	22407	Cyticine
8	9651	Galanthamine
9	8765	Physostigmine
S.No	CID	Antagonists
10	3604	Hexamethonium
11	9714	Mecamylamine
12	586269	4-(N-Maleimido)benzyltrimethylammonium
13	586270	4-(N-Maleimido)phenyltrimethylammonium
14	9778	Phencyclidine
15	222907	Dihydro-beta-erythroidine
16	108179	Lophotoxin
17	6000	d-Tubocurarine

Table 2 Sequences of α_2, α_3, α_4, α_7 and α_9 homologues of neuronal nAChRs retrieved form SwissProt (http://www.expasy.ch/sprot/) for evolutionary trace analysis

S.No	α_2		α_3		α_4		α_7		α_9	
	Source	Swissprot Id	Source	Swissprot Id	Source	Swissprot Id	Source	Swissprot Id	Source	Swissprot Id
1	HUMAN	Q15822	HUMAN	P32297	HUMAN	P43681	HUMAN	P36544	HUMAN	Q9UGM1
2	RAT	P12389	RAT	P04757	RAT	P09483	RAT	Q05941	RAT	P43144
3	MOUSE	Q91X60	MOUSE	Q8R4G9	MOUSE	O70174	MOUSE	P49582		
4	CHICK	P09480	CHICK	P09481	CHICK	P09482	CHICK	P22770	CHICK	Q9PTS8
5	PANTR	Q5IS52	BOVIN	Q07263	PANTR	Q5IS77	BOVIN	P54131		
6			CARAU	P18845	MUSPF	Q19AE6	MACMU	Q866A2		

Genetic algorithm (GA) docking was applied for 100 docking poses. All these small molecules bound to α_7nAChR were examined for their binding energy and also for specific and non-specific interacting residues. Molecules with poor binding energy were not considered for further analysis. Previously, for other membrane-bound proteins [19], a docking energy value lesser than −4 kcal mol^{-1} was considered as the weakest binding energy, and a similar threshold or filter was used to recognize good docking poses in the current docking analysis.

The ligands were again docked using AUTODOCK with α_7nAChR, keeping the ligand non-rotatable (frozen) by reducing the torsion angle freedom to zero. The same protocol was followed for subsequent consecutive dockings. The α_7nAChR–ligand bound complex was examined for specific and non-specific residues. The non-specific residues, which appear to be common for all docking, were considered as class-specific residues. Those residues were mapped on the sequence alignment and mutated on the theoretical model of α_7nAChR. The theoretical model was subjected to three different types of mutation based on the properties of the residues. These three different mutated models were subjected to energy minimization to reduce geometrical inaccuracies occurring as a result of the mutations.

The mutated models were now subjected to rigid docking using AUTODOCK. All three different mutated theoretical models, complexed with ligands, were examined for the interaction of the mutated (non-specific) residues with the ligands. The ligand-bound complexes were analyzed for bonded (H-bond) and non-bonded interaction using the in-house program Interactor (R.S., unpublished results) and AUTODOCK and compared with the wild type complexes.

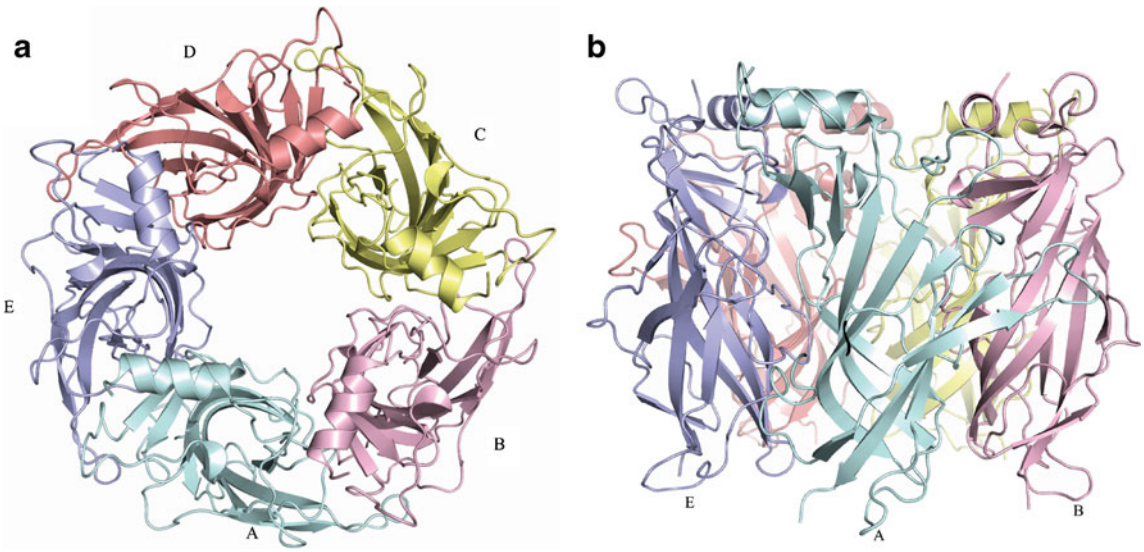

Fig. 1 **a** Theoretical model of pentameric human neuronal α_7 nicotinic acetylcholine receptor (α_7nAChR; **a**), with each subunit represented in a different color. Subunits are labeled anti-clockwise, with A–B, B–C, C–D, D–E and E–A forming the + and − chain. This forms the principle and the complementary ligand binding sites, respectively. **b** nAChR pentamer perpendicular to the fivefold axis. The ligand binding sites are located equatorially and are highlighted in different colors

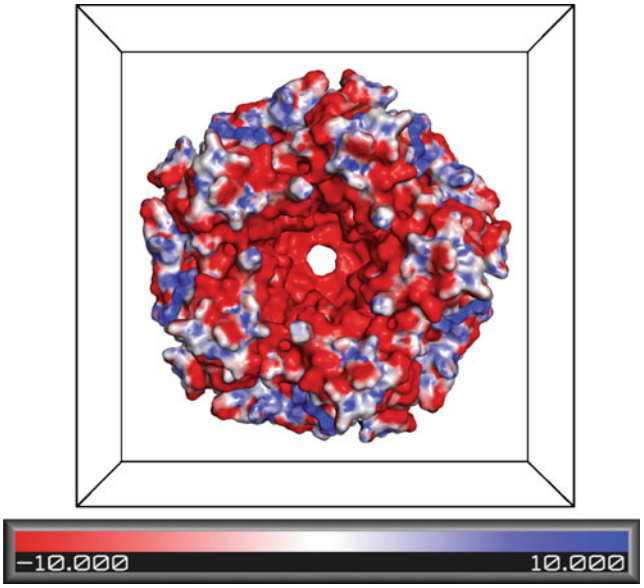

Fig. 2 Electrostatic potential map showing that the interior of the ion channel pentameric α_7nAChR is highly negative. The potential map was rendered using PyMol

Evolutionary trace analysis

Homologous protein sequences of nicotinic nAChRs (Table 2) were retrieved from UniProtKB/Swiss-Prot [20]. All these homologous sequences were subjected to evolutionary trace analysis, which was performed using the TraceSuite II server [21].

This eventually distributes the sequences into ten different partitions (P01–P10) over the phylogenetic tree in order to increase the evolutionary trace cutoff (ETC) value using the function "TraceGroups". For each partition, a trace procedure was completed automatically by the following steps: (1) protein sequences connected by a common node with an evolutionary time greater than the given ETC were clustered together; (2) a consensus was generated for each group to distinguish between conserved and non-conserved positions; (3) a trace was generated by comparing the aligned consensus sequences for all the clusters associated with a given partition. Thus, residues were classified into three types: conserved, class-specific and neutral.

Residues that are important for function, but contribute more to the functional specificity of a particular subgroup of proteins in the family are likely to be conserved, but not

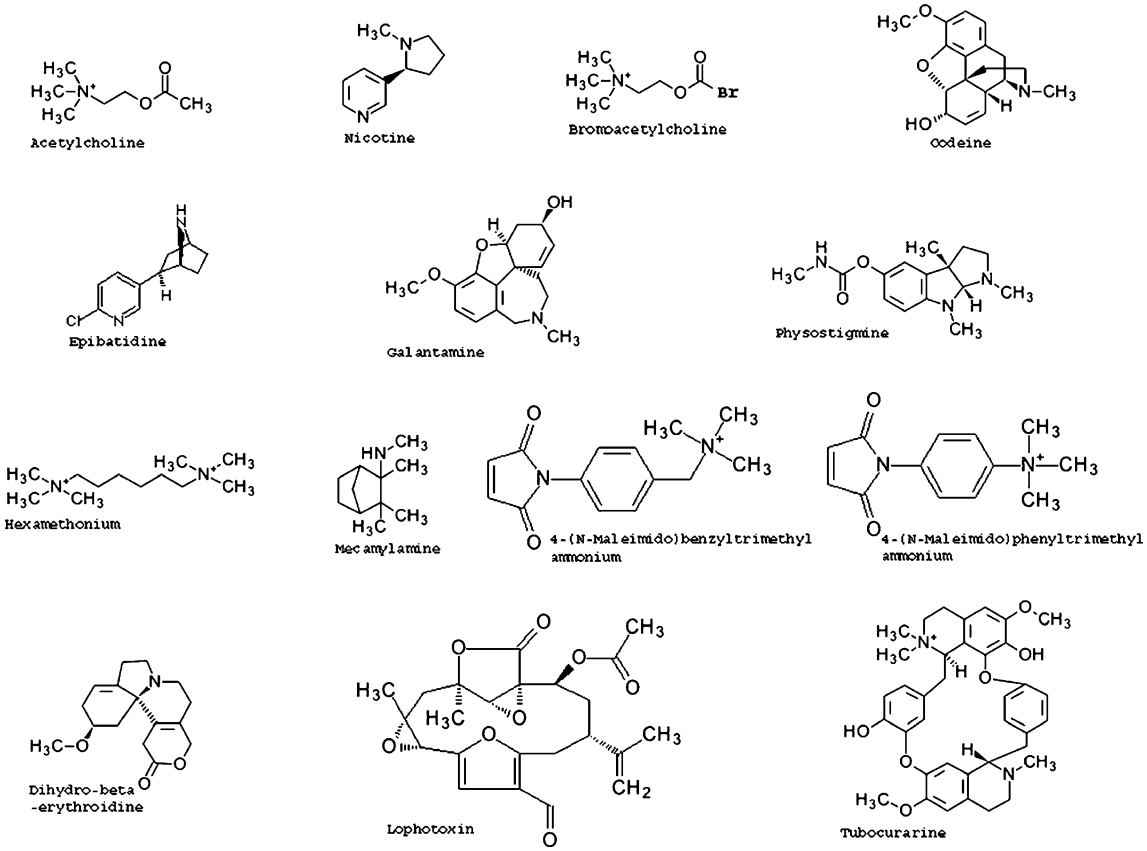

Fig. 3 Ligands (grouped into agonists and antagonists) used for docking studies with the theoretical model of α_7nAChR. For details see Table 1

invariant. Therefore, even though they might undergo mutations, the rate of mutation is still minimal. The class-specific residue denotes residues occupying a strictly conserved location in the sequence alignment, but differing in the nature of their conservation between various subgroups. This information obtained by the ET method can then be mapped on to the known protein structures, thus allowing us to identify clusters of important amino acids and to distinguish between buried and exposed residues.

By comparing the consensus, a 'trace' is generated briefly for groups of proteins that originate from a common node in a phylogenetic tree and are characterized by a common ETC.

Results and discussion

Theoretical model

In our previous studies, theoretical modeling of α_7nAChR was performed in detail. The sequence of the LBD of α_7nAChR was retrieved from SwissProt and homology modeling was performed using the crystal structure of

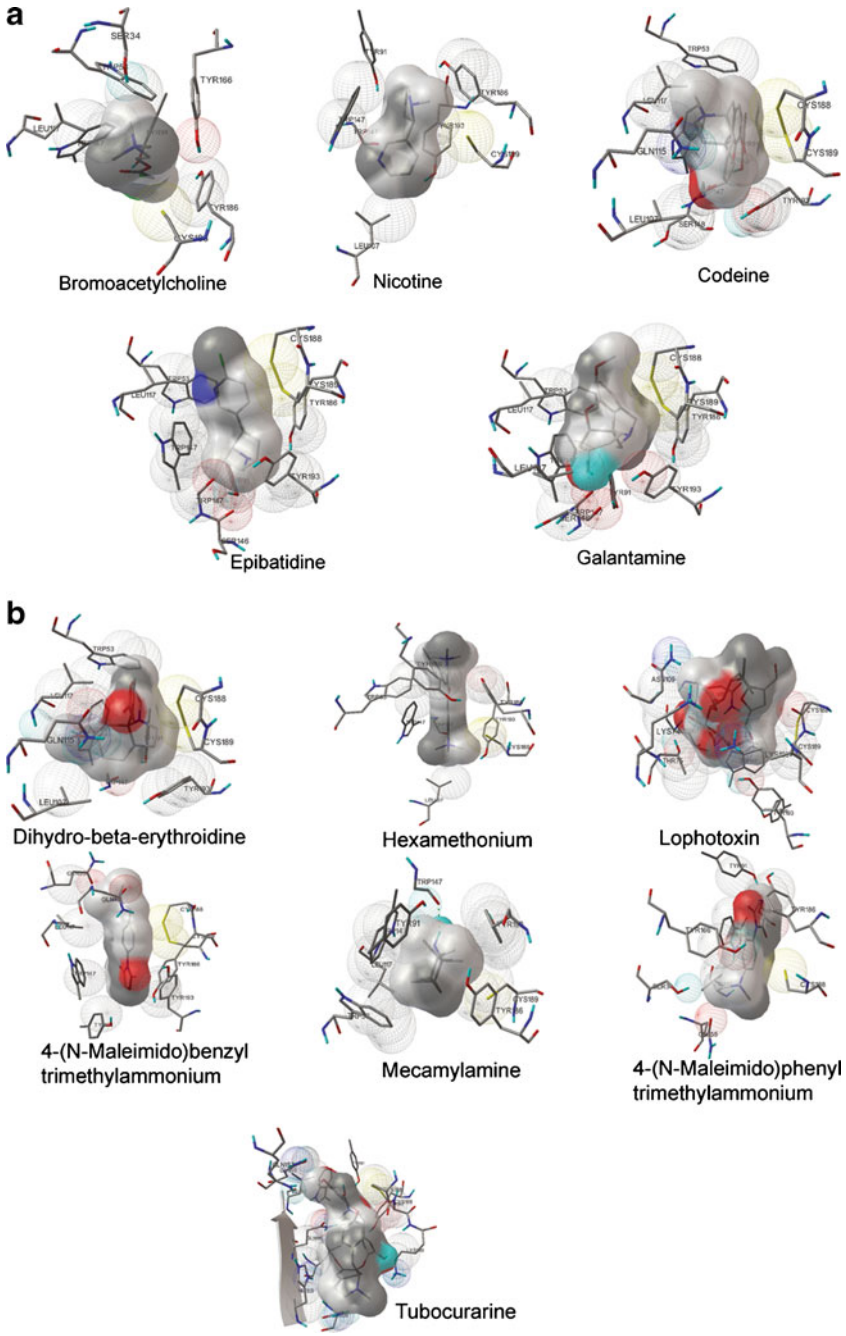

Fig. 4 Rigid ligand interactions studies on α_7nAChR. **a** Agonists interacting with the α_7nAChR. **b** Antagonists interacting with α_7nAChR. Interactions were obtained from the inbuilt module from AutoDock. For details see Table 3

AChBP (PDB ID: 1I9B) from snail as the structural template. The 1I9B structure is refined at 2.7 Å resolution and the sequence of α_7nAChR, which shares about 22.4% identity with the template, was aligned using EBI-align. Moreover, there was good agreement between the secondary structural elements of both sequences in the crucial regions. The alignment was further improved by JalView [22], a java-based alignment editor. This alignment was used for construction of the theoretical structure of α_7nAChR using Modeller9v2. This produced 20 individual models, of which only one representative structure with minimum energy was selected. Based on the initial equivalencies from the EBI-Dalilite server, the theoretical subunit was assembled into a pentamer using InsightII and subsequently minimized using Sybyl7.1 up to 100 iterations to remove the steric clashes at the interfaces. The theoretical structure was examined for structurally variable regions (SVRs) and structurally conserved regions (SCRs), highlighting regions of similarity between AChBP with α_7nAChR (Fig. 1a,b). The electrostatic potential map from PyMol shows the channel as highly cationic in nature (Fig. 2). Using this template, molecular docking studies were performed with a collection of small agonist and antagonist molecules [15].

Protein-ligand docking studies on α_7nAChR

All small molecules thought to be agonists and antagonists of α_7nAChR were retrieved from the PubChem database (Fig. 3) and treated as described in Materials and methods before subjecting them to docking. A typical docking study was carried out on the theoretical structure of α_7nAChR based on our previous studies with its agonists and antagonists. Only two protomer coordinates of α_7nAChR, which are relevant for ligand binding, were employed for docking. The docking was performed using "protein and flexible-ligand" and "protein and rigid-ligand" modes to enhance the sampling space of protein–ligand interactions (Fig. 4a,b). In the case of flexible-ligand interactions, the torsion angles of the ligands were allowed to rotate freely, while on the other hand the torsion angles of the ligands were kept rigid in rigid-ligand interactions (Table 3). By specifying the binding site locations, the search time can be significantly reduced. Thus, a grid is positioned at −14.699

Table 3 Interacting residues obtained from neuronal α_7nAChR. Flexible ligand docking was performed using Autodock4.0. The energy calculations and the interacting residues were picked out using the inbuilt module in AutoDock 4.0

S.No	Ligand	Energy (kcal/mol)	Interacting Residues
Agonist docking studies			
1	Acetylcholine	−3.58	Tyr91, Ser146, Trp147, Tyr186, Cys188, Cys189, Tyr193, Trp53, Leu117
2	Nicotine	−4.13	Tyr91, Ser146, Trp147, Ser148, Tyr186, Cys188, Cys189, Tyr193, Trp53, Leu107, Leu117, Tyr116
3	Acetylcholine Mustard	−2.47	Cys189, Tyr166, Ser34, Leu117, Trp53, Trp147
4	Bromoacetylcholine	−4.09	Gln115, Leu117, Trp147, Tyr193, Cys189, Lys190
5	Carbamylcholine	−0.99	Trp147, Leu107, Leu117, Gln115, Cys188, Cys189
6	Codeine	−4.27	Cys188, Lys190, His113, Asn109, Val108, Leu107
7	Epibatidine	−4.81	Trp147, TYR186, CYS188, CYS189, TYR166, GLN115, LEU117, LEU109
8	Cyticine	−5.86	Trp53, Leu117, Trp147, Tyr166, Cys189
9	Galanthamide	−4.63	Asn109, His113, Leu107, Lys190, Thr75, Gln115
10	Physostigmine	−3.85	Ala161, Tyr166, Tyr86, Arg184, Gly187
Antagonist docking studies			
11	Hexamethonium	−4.35	Cys189,Tyr193, Trp143, Trp53, Ley117, Gln115, Leu107
12	Serotonin	−3.92	Trp117, Cys189, Cys188, Tyr166, Glu115, Leu107, Trp53, Ser34
13	Mecamylamine	−4.35	Cys188, Cys189, Tyr193, Trp147, Leu117, Glu115, Leu107
14	4-(N-Maleimido)benzyltrimethylammonium	−6.99	Cys188, Cys189, Glu55, Tyr166, Leu117, Gln115, Leu 107, Trp147
15	4-(N-Maleimido)phenyltrimethylammonium	−6.64	Cys188, Cys189, Gln55, Glu115, Leu107, Ser148, Trp147, Leu117, Ser34, Tyr166
16	Phencyclidine	−6.07	Cys188, Cys189, Tyr193, Trp147, Leu117, Gln115
17	dihydro-beta-erythroiodine	−3.70	Tyr147, Tyr186, Cys188, Cys189, Tyr166, Gln115, Leu117, Leu109
18	Lophotoxin	−5.86	His113, Asn109, Thr75, Lys118, Lys190, Ser148
19	d-Tubocurarine	−6.92	Thr75, Gln115, Leu107, Lys74, His113, Phe185, Lys190, Lys74, Cys188, Cys190, Glu189

Table 4 Rigid ligand interaction studies. Ligands showing the best binding energies from previous docking were selected, and docking was repeated with the torsion (rigid) of the ligand reduced to zero. Binding energies were found to correlate very well with previous results

S.No	Agonist	Energy Kcal/Mol	Interacting residues
1	Bromoacetylcholine	−6.34	Ser34[a], Trp53, Let117, Tyr116[a], Tyr186,Cys188
2	Nicotine	−9.11	Leu107[a] Trp147, Tyr186, Cys189, Tyr193
3	Codeine	−10.40	Trp53, Ley107[a], Gln115,[a] Leu117, Trp147, Ser148[a], Cys188, Cys189, Tyr193
4	Epibatidine	−9.46	Trp53[a], Leu117[a], Ser146, Trp147, Tyr186[a], Cys188[a], Cys189[a], Tyr193[a]
5	Galanthamine	−10.56	Leu107, Leu117, Trp147[a], Ser148, Tyr186[a], Cys188[a], Cys189[a], Tyr193[a]
	Antagonist		
6	Hexamethionium	−6.25	Trp53[a], Leu107, Trp147,[a] Tyr166, Tyr186[a], Cys189[a], Tyr193[a]
7	Mecalamine	−10.08	Trp53[a], Leu117[a], Trp147[a], Tyr186[a], Cys189[a], Tyr193[a]
8	4-(N-Maleimido)benzyltrimethylammonium	−8.37	Gln55, Gln115, Leu117[a], Tyr186[a], Cys186[a], Cys188[a], Cys189[a], Tyr193[a]
9	4-(N-Maleimido)phenyltrimethylammonium	−8.93	Ser34, Trp53[a], Gln55, Trp147[a], Tyr166, Cys188, Tyr193[a]
10	dihydro-beta-erythroiodine	−9.47	Trp53[a], Leu107, Gln115, Leu117[a], Trp147[a], Cys188[a], Cys189[a], Tyr193[a]
11	Lophotoxin	−8.36	Trp53[a], Leu107, Gln115, Leu117[a], Trp147[a], Ser148, Tyr166, Cys188[a], Cys189[a], Tyr193[a]
12	d-Tubocurarine	−7.84	Gln55, Leu107, Asn109, His113, Gln115, Leu117[a], Gln157, Cys188[a], Cys189[a], Lys190, Tyr193[a]

[a] Key conserved residues found to interact with nAChRs (most are hydrophobic)

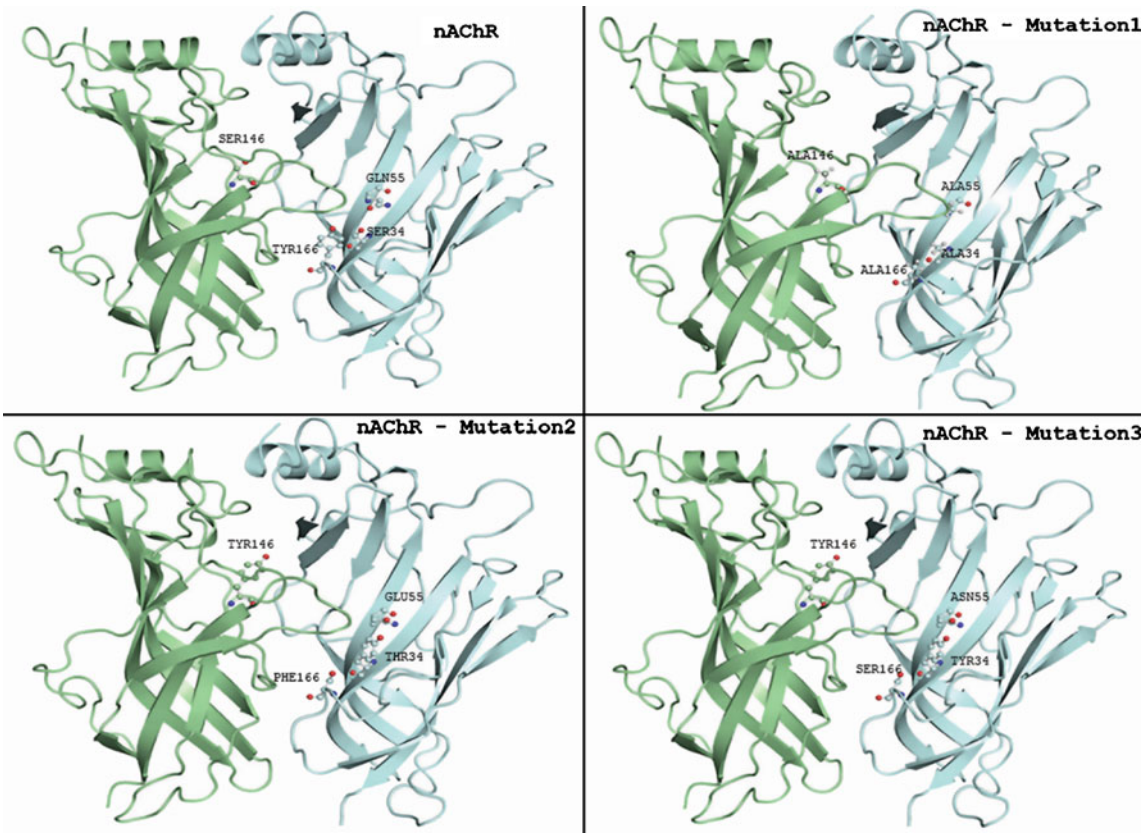

Fig. 5 nAChR and three mutant models selected for docking studies. The theoretical model was subjected to mutation based on the interaction of class-specific residues. Mutations were carried out in three different groups and based on residue properties. For details see text

Å×−26.356 Å×−3.099 Å between the interface region of the theoretical structure of α_7nAChR, which is considered to be the active site of the receptor, and also by providing a rotational space of about 0.536 Å. The docking calculations were carried out for 100 docking poses for each ligand.

The outputs from the docking of 100 GA runs were ranked according to the binding energy and clustering histogram. The scoring functions are based on protein–ligand energy terms, namely van der Waals energy, distance between the interacting atoms, dissolving energy, electrostatic energy, torsion free energy and unbound system energy. AutoDock has an inbuilt clustering method based on root mean square deviation (RMSD) values, which is used for clustering ligand poses with clustering of RMSD of >0.04 Å. According to the binding energy, the top-scoring energy for each of the ligands, and sometimes the highly populated clusters, were considered as the best ligand poses (Table 4). The analysis of the docked complex showed a drastic conformational change for cyticine and phenylcyclidine, albeit giving better binding energy after docking. Since it was difficult to interpret these data, these molecules could not be considered further for analysis.

The protein-rigid ligand interaction shows best binding energy and more highly populated clusters than the protein-flexible ligand interaction, and was thus preferred for the analysis and further study. Ligands showing very low binding energy and improper cluster formation were neglected because of the difficulty in inferring any information from

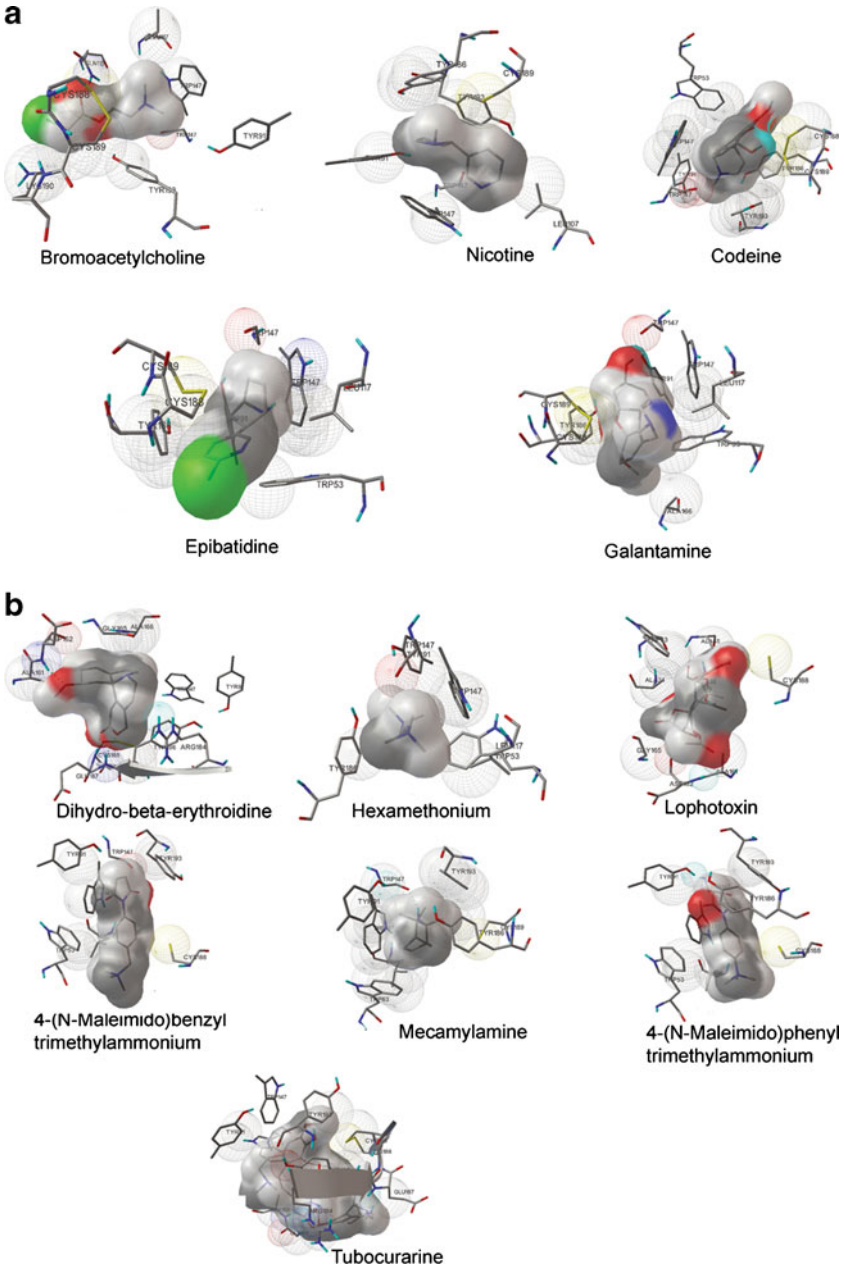

Fig. 6 Rigid ligand interaction studies on mutated α_7nAChR. **a** Agonists interacting with mutated α_7nAChR. **b** Antagonists interacting with mutated α_7nAChR. For more details see Table 5

these interactions. The complexes were analyzed for bonded and non-bonded interactions using AutoDock inbuilt modules and with our in-house program Interactor. The functional channel of the receptor molecule was contributed by charged residues for effective agonist binding. In the docking analysis, most of the small molecules were found to interact with the cysteine residues (188–189) at the binding pocket, which is dominated by hydrophobic and aromatic residues. The efficient docking analysis revealed that this core was dominated by aromatic and hydrophobic residues, contributing Tyr91, Trp147, Tyr149, Tyr186, Cys188–189 and Tyr193 to form the principle side and the complementary residues Trp53, Glu55, Leu107, Asn109, Gln115, Leu117 and Tyr166 to form the other side; this arrangement was common to the docking poses of all the ligands.

Point mutation of α_7nAChR

Potentially new interactions that were suggested due to the docking studies were mapped on the alignment of α_7nAChR and its close homologue. The new residues involved were Ser34 (−), Gln55 (−), Ser146 (+), and Tyr166 (−), and we aimed to explore more about these conserved and class-specific residues among α_7nAChR homologues (Fig. 5). These residues are highly conserved among these homologues. Given their high degree of conservation, and that they interact strongly with the ligand, it was expected that mutation of these residues would prove informative. These new residues were mutated by three different approaches based on their respective properties: (1) Ser34 of the (−) chain was replaced by Ala, Thr or Tyr; (2) Gln55 of the (−) chain was substituted with Ala, Glu or Asn; (3) Ser146 of the (+) chain was mutated to Ala, Thr and Tyr, and finally (4) Tyr166 of the (−) chain was mutated to Ala, Phe or Ser, respectively using SYBYL7.1. The mutated theoretical α_7nAChRs were subsequently energy minimized to reduce steric clashes and geometric inaccuracies occurring due to induced point residue mutations using the TRIPOS force field. This reduces the distorted energy that occurs due to residue point mutations in α_7nAChR, which was represented as an energetically stable and favorable structure for analysis. Since these three mutant models were found to be structurally stable at the end of the minimization, the structure was not greatly altered compared with the template AChBP, and so these three mutant models were selected for docking studies.

Protein-ligand docking studies on residue point mutations in α_7nAChR

Docking was carried out for these three different mutated α_7nAChR structures by applying the same procedure as above, i.e., keeping the ligand rigid for 100 cycles. The docking produces clusters of ligands interacting with α_7nAChR with high binding energy. The three different mutation-induced structures of α_7nAChR were docked using the rigid ligand approach with each ligand. The best docking poses were subjected to analysis for interacting residues within AutoDock.

Mutation 1

In the first type of mutation, all the newly interacting residues were replaced by Ala to test the effect of Ala on all

Table 5 Mutation 1. Class-specific residues identified using docking were subjected to mutation type 1. The mutation involves substitution of Ser146 (+), Ser34 (−), Gln55 (−) and Tyr166 (−) with Ala using Sybyl 7.1

S.No	Agonist	Energy (kcal/mol)	Interacting residues
1	Bromoacetylcholine	−6.12	Gln115, Leu117, Trp147, Cys188, Cys189, Lys190, Tyr193
2	Nicotine	−8.98	Leu107, Trp147, Tyr186, Cys189, Tyr193
3	Codeine	−10.40	Trp53, Tyr186, Trp147, Cys188, Cys189, Tyr193
4	Epibatidine	−9.36	Trp53, Leu117, Trp147, Tyr186, Cys188, Cys189
5	Galanthamine	−9.36	Trp53, Leu107, Gln115, Leu117, Trp147, Cys188, Cys189, Tyr193
	Antagonist		
6	Hexamethionium	−6.03	Trp53, Tyr147, Tyr186, Cys189, Tyr193
7	Mecalamine	−9.87	Trp53, Leu117, Trp147, Tyr186, Cys189, Tyr193
8	4-(N-Maleimido)benzyltrimethylammonium	−8.03	Trp53, Leu117, Trp147, Cys188, Tyr193
9	4-(N-Maleimido)phenyltrimethylammonium	−8.35	Trp53, Leu117, Trp147, Tyr186, Cys188, Tyr193
10	dihydro-beta-erythroiodine	−8.84	Leu107, Asn109, His113, Gln115, Cys188, Lys190
11	Lophotoxin	−10.73	Ser32, Ala34[a], Trp53, Ala55[a], Ala161, Asp162, Gly165, Cys188
12	D-Tubocurarine	−9.72	Trp53, Ala161, Ala166[a], Gly165, Arg184, Tyr186, Glu187, Cys188, Cys189, Tyr193

[a] Mutated residues

the subsequent rigid docking with the ligands. The docking complexes were analyzed for interacting residues with the ligands using AUTODOCK (Fig. 6a,b). Since Ala has a smaller side chain, this residue appeared in very few docking complexes (Table 5). The docking complexes were subjected to H-bond analysis using the in-house program Interactor. This program strips out residues that have hydrogen bond interactions with the ligands. In this analysis, no H-bond formation is observed with the ligand and receptor (Table 8). The docking result shows this mutant to be less effective in terms of binding energy and cluster formation. Hence, it is suggested that this mutation and its docking is not very effective in binding with ligands and further suggests that it may not be appropriate to induce an Ala mutation at any of these sites.

Mutation 2

In the second type of mutation, Ser34 (−) was replaced with Thr, Gln55 (−) was replaced with Glu, Ser146 (+) chain was replaced with Thr, and Tyr166 (−) was replaced with Phe. The docking result revealed good binding energy and good cluster formation when compared with the first type of mutation. When the complexes were analyzed for interaction using AUTODOCK (Fig. 7a,b), the Gly55-mutant model harbors many types of interaction and Cys

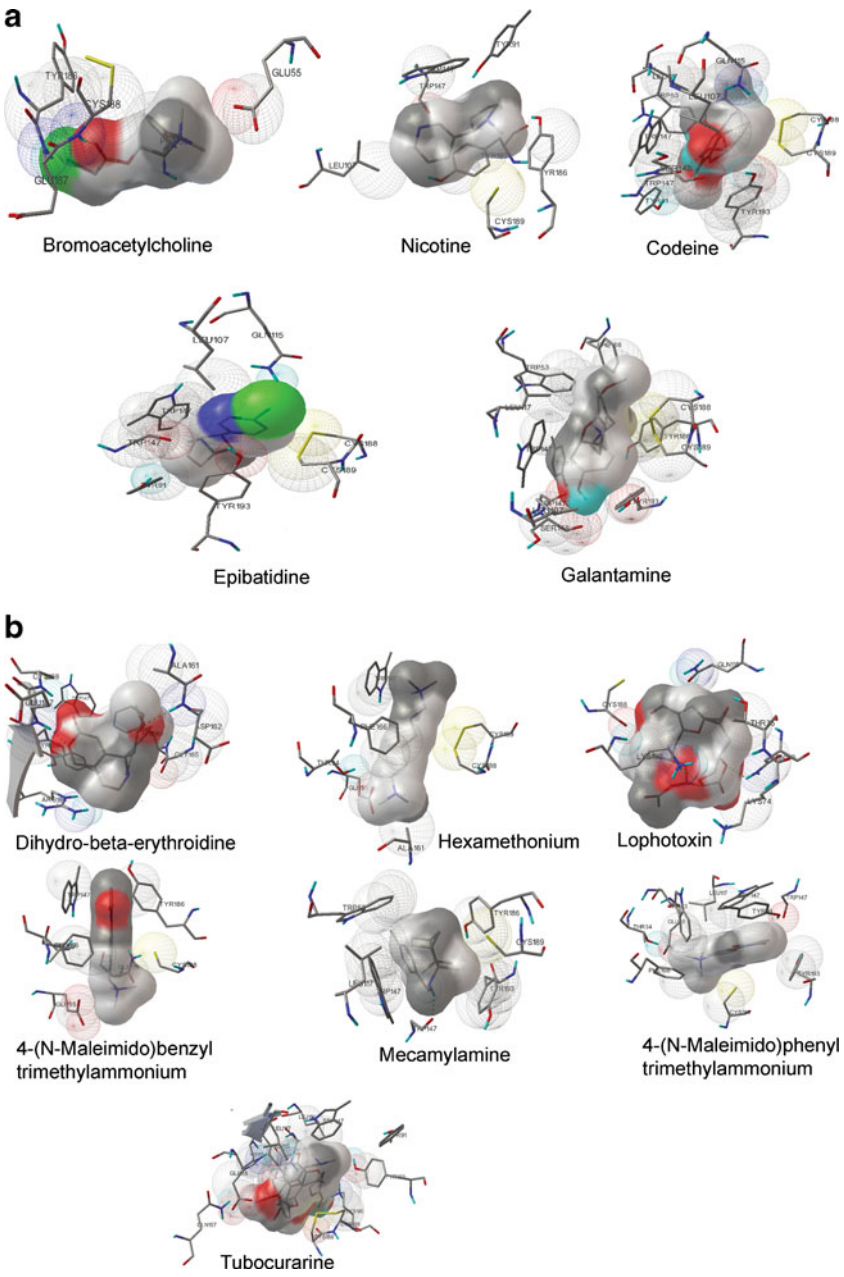

Fig. 7 Rigid ligand interaction studies on mutated α_7nAChR. **a** Agonists interacting with mutated α_7nAChR. **b** Antagonists interacting with mutated α_7nAChR. For more details see Table 6

Table 6 Mutation 2. Class-specific residues identified using docking were subjected to mutation type 2. The mutation involves substitution of Ser146 (+) with Thr, Ser34 (−) with Thr, Gln55 (−) with Glu and Tyr166 (−) with Phe using Sybyl 7.1

S.No	Agonist	Energy (kcal/mol)	Interacting residues
1	Bromoacetylcholine	−6.78	Glu55 [a], Phe166, Tyr186, Glu187, Cys188
2	Nicotine	−9.14	Leu107, Trp147, Tyr186, Cys189, Tyr193
3	Codeine	−10.36	Trp53, Leu107, Gln115, Leu117, Trp147, Ser148, Cys188, Cys189, Tyr193
4	Epibatidine	−9.43	Trp53, Phe116, Leu117, Thr146 [a], Trp147, Tyr186, Cys188, Cys189, Tyr193
5	Galanthamine	−10.62	Trp53, Leu107, Leu117, Trp147, Ser148, Tyr186, Cys188, Cys189, Tyr193
	Antagonist		
6	Hexamethionium	−6.71	Glu55 [a], Phe166, Tyr186, Cys188, Cys189, Tyr193
7	Mecalamine	−10.19	Trp53, Trp147, Tyr186, Cys189, Tyr193
8	4-(N-Maleimido)benzyltrimethylammonium	−9.00	Glu55 [a], Gln115, Leu117, Phe166, Tyr186, Cys188
9	4-(N-Maleimido)phenyltrimethylammonium	−9.36	Glu55 [a], Leu117, Phe166, Tyr186, Cys188
10	dihydro-beta-erythroiodine	−9.06	Ala161, Asp162, Gly165, Tyr166, Arg184, Tyr186, Glu187, Cys188
11	Lophotoxin	−9.54	Lys74, Thr75, Leu107, Asn109, Gln115, Cys188, Cys189, Lys190, Tyr193
12	D-Tubocurarine	−4.80	Glu55 [a], Leu107, Asn109, His113, Gln115, Leu117, Cys188, Cys189, Lys190, Tyr193

[a] Mutated residues

188–189 was found to be within interacting distance of all the ligands (Table 6). The docking complexes were subjected to our in-house program Interactor, which particularly displays H-bond interacting residues. This highlighted Glu55, which has an H-bond interaction with the ligand molecule (Table 8). This confirms the result that this docking is pretty effective for ligand binding, further suggesting that Q55 (−) E is not likely to change the activity of the protein.

Mutation 3

In the third type of mutation, Ser34 (−) was replaced with Tyr, Gln55 (−) was replaced with Asn, Ser146 (+) chain was replaced with Tyr, and Tyr166 (−) was replaced with Ser. The docking result indicated good binding energy and good cluster formation when compared with the other two types of mutation. The complexes were subsequently subjected to analysis of the interacting residues using AUTODOCK (Fig. 8a,b). Tyr146 and Ser166 appear within ligand-interacting distance in many of the antagonists. Also, Cys 188–189 was found to be involved in interaction with the ligand in all cases (Table 7). When the docked complexes were subjected to Interactor, H-bond interactions were displayed with Tyr146 and Ser166 in some cases (Table 8). This result confirms that this docking is very effective in ligand binding, particularly to antagonists. This also suggests that the α_7nAChR is highly sensitive to these antagonists. These mutation investigations could be subjected to further experimental study, to validate and use such results in an effective manner in future. These results provide details of the interactions of ligands with the three dimensional model of the N-terminal region of human α_7nAChR, thereby also suggesting strategies for the design of novel lead compounds [24].

Evolutionary trace analysis

In order to examine the impact of mutations of residues in conserved and class-specific regions of nAChR, a series of diverse nAChR receptors needs to be tested. Evolutionary trace (ET) analysis—a sequence-structure analysis technique [23]—was applied to identify potential regions for mutagenesis in nAChR. ET analysis aims to find determinants of receptor binding specificity for the five major subgroups in the nAChR family by creating an evolutionary tree using the PHYLIP package. The ECD of α_2, α_3, α_4, α_7 and α_9 sequences of the nAChR family were retrieved from the SwissProt database and submitted to the Trace Suite II server. The complete sequences of these polypeptides were aligned manually, using the invariant cysteines of nAChR as anchor points. Special care was taken to ensure that gaps were not inserted into areas of known secondary structure. A Phylip distance matrix based on sequence identity was generated using the program ClustalX from the 26 non-redundant sequences (Table 9), and was used as input in the Kitsch algorithm to build a rooted phylogenetic tree. The server produces both a phylogenetic tree and a trace

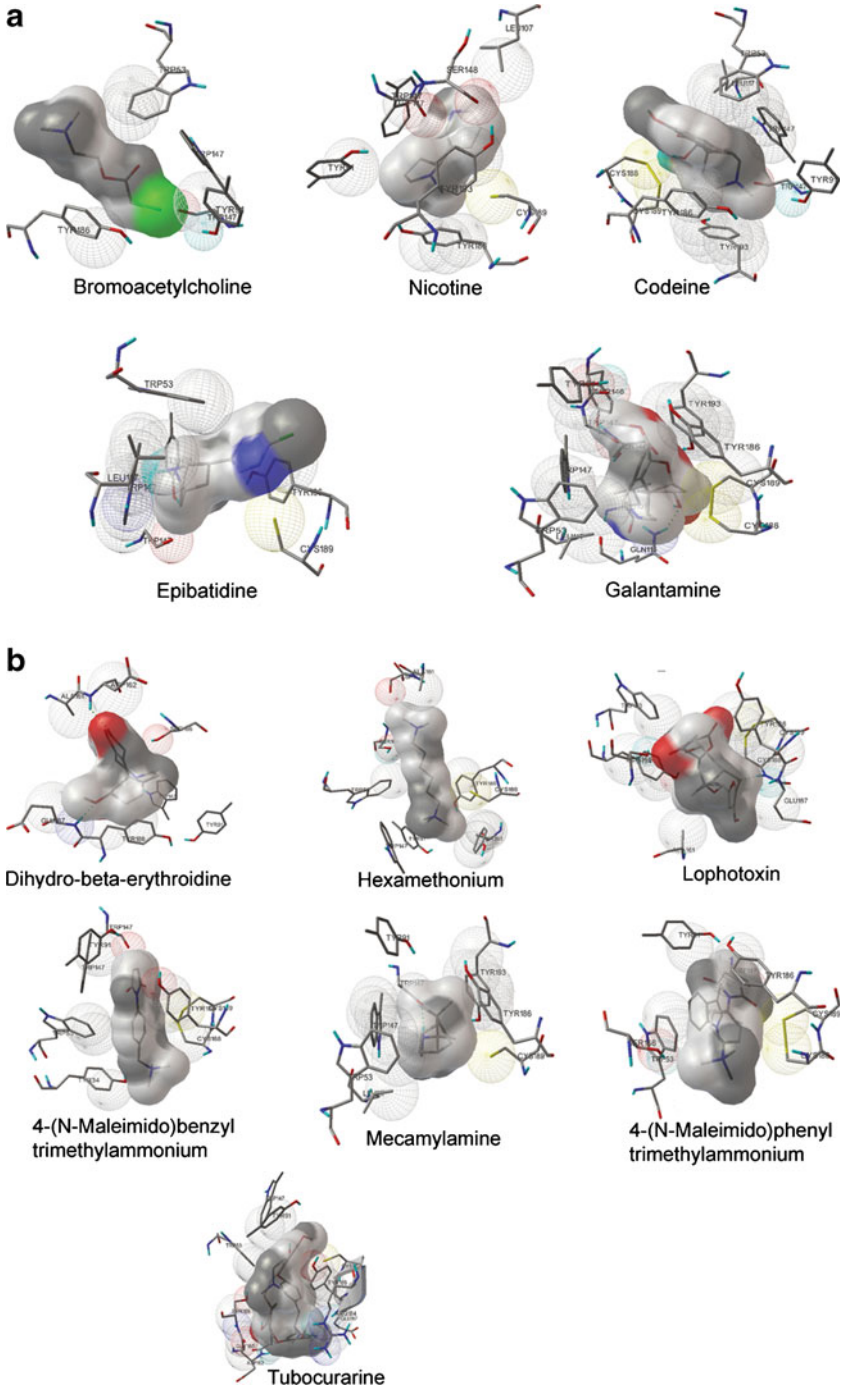

Fig. 8 Rigid ligand interaction studies on mutated α_7nAChR. **a** Agonists interacting with mutated α_7nAChR. **b** Antagonists interacting with mutated α_7nAChR. For more details see Table 7

alignment. The trace alignment produces ten consensus sequences at each level of ETC, and the phylogenetic tree is generated from five major branches with partitions ranging from P1 to P10. As expected, the sequence from *Lymnaea stagnalis* stands on its own as a separate cluster and the nAChR sequences were found to be more similar.

For each partition, the trace procedure was followed automatically by TraceSeq and TraceScript, using the following sequence of steps: (1) protein sequences connected by a common node with an evolutionary time greater than a given ETC value were clustered together by TraceGroup and input into TraceSeq. (2) To distinguish between conserved and non-conserved positions, a consensus sequence was generated for each group. In practice, TraceSeq tagged a residue with '1' if it was conserved or with '0' if it varied within the subgroup. (3) By comparing the aligned consensus sequences for all the clusters associated with a given partition, a trace was generated. Where all residues for a specific position had been tagged as '1', the one-letter residue name was used if such an

Table 7 Mutation 3. Class-specific residues identified using docking were subjected to mutation type 3. This mutation involves substitution of Ser146 (+) with Tyr, Ser34 (−) with Tyr, Gln55 (−) with Asn and Tyr166 (−) with Ser using Sybyl 7.1. The results were obtained using the inbuilt module for analyzing the interacting residues in AutoDock

S.No	Agonist	Energy (kcal/mol)	Interacting residues
1	Bromoacetylcholine	−6.39	Leu107, Gln115, Cys189, Tyr193
2	Nicotine	−9.23	Trp147, SER148, Tyr186, Cys189, Tyr193
3	Codeine	−10.61	Trp53, Leu117, Trp147, Tyr186, Cys188, Cys189, Tyr193
4	Epibatidine	−10.01	Trp53, Leu117, Trp147, Tyr186, Cys189
5	Galanthamine	−10.64	Trp53, Leu107, Gln115, Leu117, Tyr146[a], Trp147, Ser148, Tyr186, Cys188, Cys189, Tyr193
	Antagonist		
6	Hexamethionium	−6.32	Trp53, Ala161, ASP162, Ser166[a], Tyr186, Cys189, Tyr193
7	Mecalamine	−10.06	Trp53, Leu117, Trp147, Tyr186, Cys189, Tyr193
8	4-(N-Maleimido)benzyltrimethylammonium	−8.23	Trp53, Trp147, Ser166[a], Tyr186, Cys188, Cys189
9	4-(N-Maleimido)phenyltrimethylammonium	−8.53	Trp53, Leu117, Trp147, Ser148, Ser166[a], Tyr186, Cys189
10	dihydro-beta-erythroiodine	−8.91	Ala161, Ala162, Ser166[a], Tyr186, Glu187
11	Lophotoxin	−10.48	Tyr34[a], Trp53, Tyr91, Ala161, Ser166[a], Tyr186, Glu187, Cys188, Cys189
12	d-Ttubocurarine	−10.39	Trp53, Ala161, ASP162, Gly165, Ser166[a], Arg184, Tyr186, Glu187, Cys189

[a] Mutated residues that appear to interact with the ligand

amino acid was found in every single cluster, otherwise the position was assigned the symbol 'X' and was termed 'Class-specific'; if an amino acid had been tagged with a '0' in at least one of the consensus sequences, the corresponding position in the trace was considered to be neutral. (4) Script files for both Rasmol and MOLSCRIPT were created by TraceScript to map the trace onto the surface of available structures. The various residue classes were color-coded to distinguish between conserved and class-specific, as well as buried and exposed. Residues were classified as buried if their side-chain solvent accessibility was lower than 30%.

The analysis was carried out on five different groups among the nAChR sequences in order to validate the method. The aligned non-redundant sequences of nAChR, which contains five α_2 sequences, five α_3 sequences, six α_4 sequences, six α_7 sequences, and three α_9 sequences with one AChBP sequence from *Lymnaea stagnalis*. Sequences of subfamilies show high conservation among themselves, but across subfamilies there is hardly any conservation

Table 8 H-Bond analysis using Interactor. All the docked complexes were subjected to H-bond analysis using our in-house program Interactor. The program stripped out the residues that were interacting with the respective ligand. More hydrogen bond interactions were found in mutation types 2 and 3 than with mutation type 1, thus indicating that mutation types 2 and 3 were more efficient than type 1

S.No	Ligand	Wild	M1	M2	M3
1	Bromoacetylcholine	Gln55[a]	X	Glu55	X
2	Codeine	X	X	X	X
3	dihydro-beta-erythroiodine	X	X	X	X
4	Epibatidine	X	X	X	X
5	Galanthamine	X	X	X	Tyr146
6	Hexamethionine	X	X	Glu55	X
7	Lophotoxin	X	X	X	Ser166
8	4-(N-Maleimido)benzyltrimethylammonium	X	X	Glu55	X
9	Mecalamine	X	X	X	X
10	4-(N-Maleimido)phenyltrimethylammonium	X	X	Glu55	X
11	Nicotine	X	X	X	X
12	D-Tubocurarine	Gln55	Ala166	Glu55	Ser166

[a] X represents no H-bond interaction and the residue name indicates interaction of the ligand with that residue

Table 9 Conserved, class-specific and neutral residues in the extracellular region of nAChR, generated based on the trace produced by the Evolutionary Trace Server. Around 26.6% of residues are conserved among the homologous sequences

S.No		Alpha7[a]	Alpha9[a]	Alpha2[b]	Alpha3[b]	Alpha4[b]
1	5	L	L	L	L	L
	6	Y	F	F	F	L
	7(B)[c]	K	N	K	E	K
	8	E	D	H	R	K
2	9	L	L	L	L	L
	10	V	F	F	F	F
	11	K	E	R	E	S
	12	N	D	G	D	G
3	13	Y	Y	Y	Y	Y
	14	N	S	N	N	N
	15(A)[c]	P	N	R	E	K
	16	L	A	W	I	W
	17(A)[c]	E	L	A	I	S
4	18(A)[c]	R	R	R	R	R
5	19(A)[c]	P	P	P	P	P
6	20	V	V	V	V	V
	21	A	P	A	A	E
	22	N	N	N	N	D
	23	D	T	V	I	T
	24	S	S	S	S	D
	25	Q	D	D	D	K
	26	P	V	P	V	V
	27	L	V	V	V	L
	28	T	I	I	L	N
	29	V	V	I	V	V
	30	Y	R	Q	R	T
	31	F	F	F	F	L
	32	S	G	E	G	Q
	33	L	L	V	L	I
	34	S	S	S	S	T
	35	L	I	M	I	L
	36	L	A	S	A	S
	37(B)[c]	Q	Q	Q	Q	Q
	38	I	I	L	L	L
	39(B)[c]	M	K	I	V	I
	40	D	D	D	K	D
	41	V	M	V	V	V
7	42	D	D	D	D	D
8	43	E	E	E	E	E
	44	K	R	K	V	K
9	45(A)[c]	N	N	N	N	N
10	46	Q	Q	Q	Q	Q
	47	V	I	M	I	M
	48	L	L	M	M	M
	49	T	T	T	E	T
	50	T	A	T	T	T
	51	N	Y	N	N	N
	52(B)[c]	I	L	V	L	V
11	53	W	W	W	W	W
	54	L	I	L	L	V
	55	Q	R	K	K	K
	56	M	Q	Q	Q	Q
	57	S	I	E	I	E
12	58	W	W	W	W	W
	59	T	H	S	N	H
13	60	D	D	D	D	D
	61	H	A	Y	Y	Y
	62	Y	Y	K	K	K
14	63	L	L	L	L	L
	64	Q	T	R	K	R
15	65	W	W	W	W	W
16	77	R	R	R	R	R
	78	F	I	V	V	P
17	79	P	P	P	P	I
	80	D	S	S	A	S
	81	G	D	E	E	E
	82	Q	L	M	K	L
	83	I	V	I	I	I
18	84	W	W	W	W	W
	85(A)[c]	K	R	I	K	R
19	86	P	P	P	P	P
20	87	D	D	D	D	D
21	88	I	I	I	I	I
	89	L	V	V	V	V
22	90	L	L	L	L	L
23	91	Y	Y	Y	Y	Y
24	92(A)[c]	N	N	N	N	N
	93(A)[c]	S	K	N	N	N
25	94(A)[c]	A	A	A	A	A
	95	D	D	D	V	D
	96	E	D	G	G	G
	97	R	E	E	D	D
	98(B)[c]	F	S	F	F	F
	99(B)[c]	D	S	A	Q	A
	100(B)[c]	A	E	V	V	V
	101	T	P	T	D	T
	102(B)[c]	F	H	D	H	V
	103	H	M	K	L	N
	104(B)[c]	T	T	T	T	T
	105	N	K	K	K	N
	106	V	A	A	A	V
	107	L	H	L	H	V
	108	V	L	L	L	L
	109	N	F	K	F	R
	110	S	S	Y	H	Y

Table 9 (continued)

S.No		Alpha7[a]	Alpha9[a]	Alpha2[b]	Alpha3[b]	Alpha4[b]
	111	S	T	T	D	D
	112	G	G	G	G	G
	113	H	T	E	R	L
	114	C	V	V	V	I
	115	Q	H	T	Q	T
	116	Y	W	W	W	W
	117	L	V	I	T	D
26	119	P	P	P	P	P
	120	G	A	A	A	A
27	121	I	I	I	I	I
	122(A)[c]	F	T	Y	F	Y
28	123	K	K	K	K	K
29	124(A)[c]	S	S	S	S	S
30	125	S	S	S	S	S
31	126	C	C	C	C	C
	127	Y	V	S	K	S
	128	I	V	I	I	I
32	129	D	D	D	D	D
33	130	V	V	V	V	V
	131	R	T	T	T	T
	132	W	Y	F	Y	F
34	133	F	F	F	F	F
35	134	P	P	P	P	P
36	135	F	F	F	F	F
37	136	D	D	D	D	D
	137	V	N	Q	Y	Q
38	138	Q	Q	Q	Q	Q
	139	H	Q	N	N	N
39	140	C	C	C	C	C
	141	K	N	K	T	T
	142	L	L	M	M	M
	143(A)[c]	K	T	K	K	K
40	144(A)[c]	F	F	F	F	F
41	145	G	G	G	G	G
42	146(A)[c]	S	S	S	S	S
43	147(A)[c]	W	W	W	W	W
	148(A)[c]	S	T	T	S	T
44	149(A)[c]	Y	Y	Y	Y	Y
	150(A)[c]	G	N	D	D	D
	151	G	G	K	K	K
	152	W	N	A	A	A
	153	S	Q	K	K	K
	154	L	V	I	I	I
	155	D	D	D	D	D
	156	L	L	L	L	I
	157	Q	E	V	V	F
	158	M	Q	L	N	N
	159	Q	M	I	M	A
	160	E	E	G	H	L
	161	A	Q	S	S	D
	–	–	T	S	R	S
	–	–	V	M	V	G
	162(B)[c]	D	D	N	D	D
	163	I	L	L	Q	L
	164	S	K	K	L	S
	165(B)[c]	G	D	D	D	D
	166	Y	Y	Y	F	F
	167	I	W	W	W	I
	168(B)[c]	P	E	E	E	E
	169	N	S	S	S	D
	170(B)	G	G	G	G	V
45	171	E	E	E	E	E
46	172	W	W	W	W	W
	173	D	A	A	V	E
	174	L	I	I	I	V
	175	V	V	I	V	H
	176	G	N	K	D	G
	177	I	A	A	A	M
	178	P	T	P	V	P
	179	G	G	G	G	A
	180	K	T	Y	T	V
	181	R	Y	K	Y	K
	182	S	N	H	N	N
	183	E	S	D	T	V
	184	R	K	I	R	I
47	185	Y	Y	Y	Y	Y
	186(A)[c]	E	G	D	N	E
48	187(A)[c]	C	C	C	C	C
49	188(A)[c]	C	C	C	C	C
	189	K	S	A	E	A
50	190	E	E	E	E	E
	191	P	P	I	I	I
51	192	Y	Y	Y	Y	Y
52	193	P	P	P	P	P
53	194	D	D	D	D	D
	195	V	V	V	I	I
54	196	T	T	T	T	T
	197	F	F	Y	Y	Y
	198	T	T	A	S	A
	199	V	L	F	L	F
	200	T	L	V	Y	V
	201	M	L	I	I	I
	202	R	K	R	R	R
	203	R	R	R	R	R

[a] Forms homopentamers

[b] Forms heteropentamer

[c] Residues at the interface region

apart from the cysteines. It should be noted that Cys188–189 is also conserved among the superfamily and in fact is said to be the hallmark of this superfamily. However, Ser146 was absolutely conserved among all subtypes. The polar residue Ser34 (already identified during docking as an interesting residue) is replaced by polar and aromatic residues present at the β_1 region that may be important for specificity of binding. It is conserved among nicotinic-type receptors but varies slightly in the muscarnic type of nAChR. In contrast, Gln55 displays maximal sequence variation among the subtypes and Tyr166 is highly conserved in nicotinic-type receptors but not in the

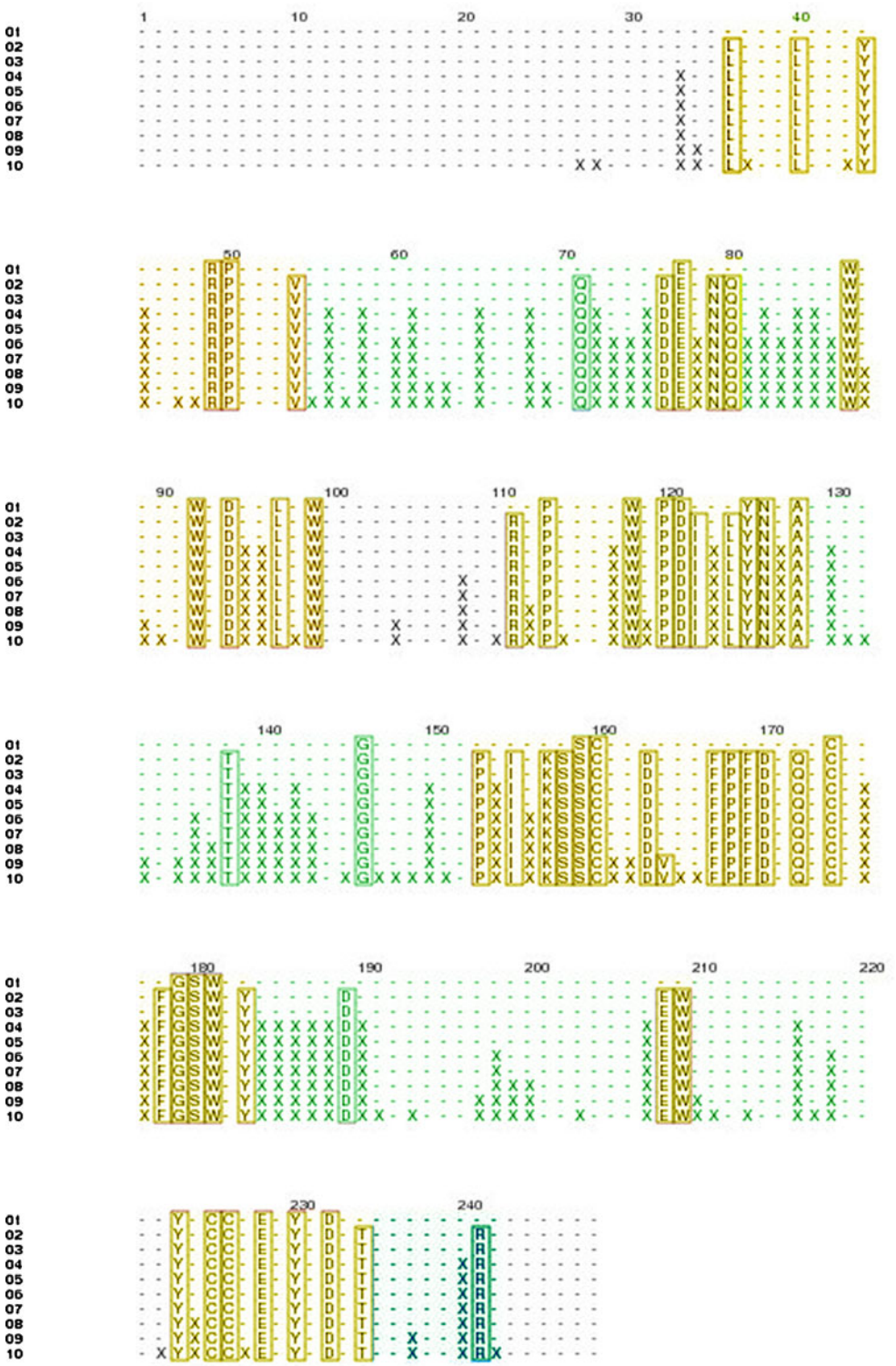

Fig. 9 Evolutionary trace (ET) analysis of nAChR. The extracellular domain of α_2, α_3, α_4, α_7 and α_9 of neuronal nAChR sequences were aligned for partition P1–P10. *Yellow* Conserved residues, *green* class-specific residues, *cyan* neutral residues

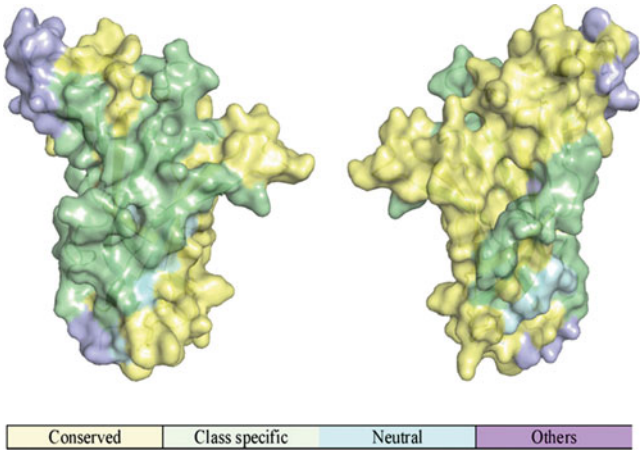

Fig. 10 Results of ET mapped over the theoretical structure of α_7nAChR. *Yellow* Conserved residues, *green* class-specific residues, *light cyan* neutral residues

muscarnic type, which display minimal sequence variation. However, the number of conserved residues among the homologous sequences was not very high since the average sequence identity was found to be only 26.6%.

The output from the TraceSuiteII program on the ECD of nAChR is shown in Fig. 9. Analysis of the mapped traces for partitions P1–P10 revealed clusters of potentially important residues in the binding site of the receptor. The residues defined by their hydrophobic trait are at the interface region. In the partition P01, apart from the structurally conserved cysteines at the interface region, the following are absolutely conserved among the receptors of nAChR: Arg18, Pro19, Glu43, Trp53, Trp58, Asp60, Leu63, Trp65, Pro79, Trp84, Pro86, Asp87, Tyr91, Asn92, Ala94, Gly112, Ser125, Cys126, Cys140, Gly145, Ser146, Trp147, Tyr186, Glu191, Tyr193 and Asp195. Among the conserved residues, Trp53, Tyr91, Trp147, Tyr186, Cys188–189 and Tyr193 were found to be involved at the interface region, which is the binding site region. The disulfide linkage Cys126–Cys140 is located between β_4 and β_7; and the Cys188–Cys189 bridge located between the loop region β_9 and β_{10} maintains the structural rigidity.

At partition P02, Leu5, Leu9, Tyr13, Val20, Gly37, Asp42, Asn45, Gln46, Leu90, Thr101, Pro119, Ile121, Lys123, Ser124, Asp129, Val130, Phe133, Pro134, Phr135, Asp136, Gln138, Phe144, Tyr149, Asp155, Gly171, Trp172, Tyr197 and Arg205 were found to be conserved among all the α_2, α_3, α_4, α_7 and α_9 nAChR types. Among the conserved residues, Glu43, Trp58, Asp60, Leu63, Trp65, Pro79, Trp84, Pro86 and Asp87, which lie away from the interface region and binding site, perhaps possess less functional importance. Residues present at the partition P04 were identified as class-specific residues. The conserved, class-specific and neutral residues identified using TraceSuite were mapped on the surface of the theoretical model nAChR (Fig. 10) to examine their spatial distribution. This ensures that the functional patches detected at the binding site of these highly related protein sequences occupy similar regions of the molecule, regardless of their functional differences.

Phylogenetic tree

The partitions ranging from P01 to P10 divide the phylogenetic tree into respective groups based on appropriate classes. An individual partition contains different numbers of classes, where each class consists of a cluster of similar sequences originating from a common node within the respective partition (Fig. 11). From the root, nodes 1 and 2 originated at the level of partition P01. One of these branches contains the AChBP sequence, while the other branch consists of the remaining nAChR sequences, indicating that the AChBP sequences may indeed constitute an independent and distinct node to nAChR. Partition P03 discriminates into node3, in which the α_9 group is collated into a single branch, and node4, which comprises the remaining α groups. However, partition P04 further divides into node5 and node6, in which α_7 sequences were grouped into a single branch, and the rest of the α_2, α_3, α_4 groups into partition P06. At partition P06, nodes 7 and 8 were further classified into α_3 group and α_2, α_4 groups, respectively. Partition P08 grouped into two different clusters of α_2, α_4 groups at the 9th and 10th node, respectively, which lie proximal to each other. Thus, the ET method can be used both to rationalize the results of

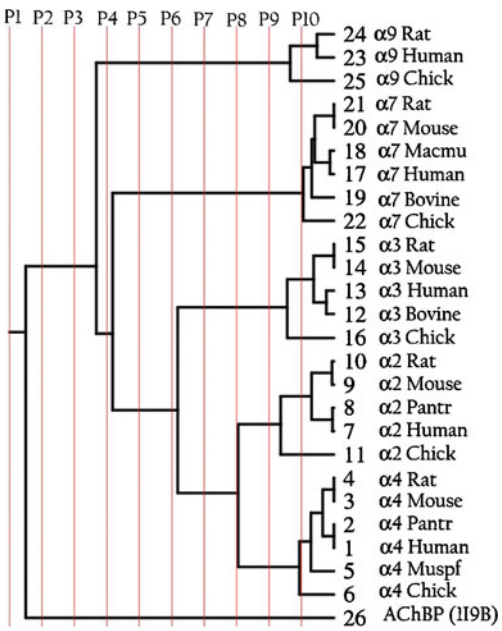

Fig. 11 Dendrogram representing 26 ECD sequences of the nAChR family, selected using Phylip 3.5 on the basis of sequence dissimilarity

mutagenesis studies and to predict novel leads for future experiments.

Conclusions

α_7nACh receptors are gaining increasing attention among the ion channels since they modulate neurotransmission at both pre- and post-synaptic junctions. Computational modeling of the interaction of relevant ligands with the theoretical model of nAChR will be of great value in the discovery of lead compounds. The theoretical model of α_7nAChR generated in our previous study was subjected to receptor-ligand docking studies. The model was generated as a monomer and assembled as a pentamer using the initial equivalences from the EBI-Dalilite server, and stereochemical clashes and structural inaccuracies were corrected by energy minimization. Thus, the structure was found to be satisfactory as assessed by various analyses [17].

Ligands corresponding to agonists and antagonists of α_7nAChR were retrieved from the PubChem database and the processed ligands were subjected to docking with the theoretical model α_7nAChR. These ligands were buried in the aromatic and hydrophobic clusters located at the interface region. Further analysis of our docking trials revealed that Ser34, Gln55, Ser146 and Tyr166 at the interface region may be expected to play an additional important role in ligand binding specificity. To our knowledge, this has not been reported elsewhere and these observations could be subject to site-directed mutations for test-of-function experiments.

The residues identified were subjected to in silico point mutagenesis and further docking studies to examine the role of these residues in ligand binding. In silico point mutagenesis experiments were therefore designed in such a way as to permit clear investigation of the contribution made by the residues at the interface region and the stability of ligand binding, as well as their contribution to the ability to interact with other proteins. The three types of mutations tested revealed the mutated class-specific residues interacting with agonists and antagonists. Subsequently, an H-bond analysis was performed using our in-house program Interactor, which revealed some interaction between antagonists and the class-specific mutated residues of the receptor.

In support of the docking studies, ET analysis was also performed on homologues of nAChRs. The ET results identified a few potential residues as the most conserved, and class-specific residues that might be important for the interaction of the receptor with agonists and antagonists. Moreover, ET analysis was found to be consistent with the above-mentioned docking studies on the receptor, suggesting similar residues as being crucial for its interaction. These residues were present at one of the loop regions and the β_1, β_2 and β_7 regions, which may interact with ligands, and were also identified by ET analysis independently, revealing good agreement with docking results.

The role played by all conserved residues and the class-specific residues highlighted in our analysis should be investigated further by experimental mutagenesis studies. Detailed studies of the five major α subunits of nicotinic nAChR subgroups enabled us to understand the role of residues involved in the interaction in the formation of nAChR-ligand complexes. Hence, it may be helpful to us in the design of therapeutic leads agents for neurodegenerative diseases.

Acknowledgements The authors (M.P. and P.S.) thank the Department of Biotechonolgy-Bioinformatics Infrastructural Facility provided at Bharathiar University, Coimbatore. We also thank the National Centre for Biological Sciences, Bangalore, for infrastructural support.

References

1. Van Rensburg R, Chazot P (2008) Alpha7 nicotinic acetylcholine receptors: molecular pharmacology and role in neuroprotection. Curr Anaesth Crit Care 19(4):202–214. doi:10.1016/j.cacc.2008.05.001
2. Changeux JP, Taly A (2008) Nicotinic receptors, allosteric proteins and medicine. Trends Mol Med 14(3):93–102. doi:10.1016/j.molmed.2008.01.001
3. Celie PH, van Rossum-Fikkert SE, van Dijk WJ, Brejc K, Smit AB, Sixma TK (2004) Nicotine and carbamylcholine binding to nicotinic acetylcholine receptors as studied in AChBP crystal structures. Neuron 41(6):907–914. doi:10.1016/S0896-6273(04)00115-1
4. Brejc K, van Dijk WJ, Klaassen RV, Schuurmans M, van Der Oost J, Smit AB, Sixma TK (2001) Crystal structure of an ACh-binding protein reveals the ligand-binding domain of nicotinic receptors. Nature 411(6835):269–276. doi:10.1038/35077011
5. Capener CE, Kim HJ, Arinaminpathy Y, Sansom MS (2002) Ion channels: structural bioinformatics and modelling. Hum Mol Genet 11(20):2425–2433
6. Harel M, Kasher R, Nicolas A, Guss JM, Balass M, Fridkin M, Smit AB, Brejc K, Sixma TK, Katchalski-Katzir E, Sussman JL, Fuchs S (2001) The binding site of acetylcholine receptor as visualized in the X-Ray structure of a complex between alpha-bungarotoxin and a mimotope peptide. Neuron 32(2):265–275. doi:10.1016/S0896-6273(01)00461-5
7. Bourne Y, Talley TT, Hansen SB, Taylor P, Marchot P (2005) Crystal structure of a Cbtx-AChBP complex reveals essential interactions between snake alpha-neurotoxins and nicotinic receptors. EMBO J 24(8):1512–1522. doi:10.1038/sj.emboj.7600620
8. Dellisanti CD, Yao Y, Stroud JC, Wang ZZ, Chen L (2007) Crystal structure of the extracellular domain of nAChR alpha1 bound to alpha-bungarotoxin at 1.94 A resolution. Nat Neurosci 10(8):953–962. doi:10.1038/nn1942
9. Unwin N (2005) Refined structure of the nicotinic acetylcholine receptor at 4A resolution. J Mol Biol 346(4):967–989. doi:10.1016/j.jmb.2004.12.031
10. Karlin A (2002) Emerging structure of the nicotinic acetylcholine receptors. Nat Rev Neurosci 3(2):102–114. doi:10.1038/nrn731
11. Schapira M, Abagyan R, Totrov M (2002) Structural model of nicotinic acetylcholine receptor isotypes bound to acetylcholine

and nicotine. BMC Struct Biol 2(1):1–8. doi:10.1186/1472-6807-2-1
12. Le Novère N, Grutter T, Changeux JP (2002) Models of the extracellular domain of the nicotinic receptors and of agonist- and Ca2+ -binding sites. Proc Natl Acad Sci USA 99(5):3210–3215. doi:10.1016/S0306-4522(00)00512-1
13. Itier V, Bertrand D (2001) Neuronal nicotinic receptors: from protein structure to function. FEBS Lett 504(3):118–125. doi:10.1016/S0014-5793(01)02702-8
14. Ivanov I, Cheng X, Sine SM, McCammon JA (2007) Barriers to ion translocation in cationic and anionic receptors from the Cys-loop family. J Am Chem Soc 129(26):8217–8224. doi:10.1021/ja070778l
15. Parthiban M, Rajasekaran MB, Ramakumar S, Shanmughavel P (2009) Molecular modeling of human pentameric alpha(7) neuronal nicotinic acetylcholine receptor and its interaction with its agonist and competitive antagonist. J Biomol Struct Dyn 26 (5):535–548. doi:10.1016/j.jmgm.2008.01.004
16. Sali A, Blundell TL (1993) Comparative protein modelling by satisfaction of spatial restraints. J Mol Biol 234(3):779–815. doi:10.1016/S1357-4310(95)91170-7
17. Holm L, Park J (2000) DaliLite workbench for protein structure comparison. Bioinformatics 16(6):566–567
18. Morris AL, MacArthur MW, Hutchinson EG, Thornton JM (1992) Stereochemical quality of protein structure coordinates. Proteins 12(4):345–364
19. Kanagarajadurai K, Malini M, Bhattacharya A, Panicker M, Sowdhamini R (2009) Molecular modeling and docking studies of human 5-hydroxytryptamine 2A (5-HT2A) receptor for the identification of hotspots for ligand binding. Mol BioSyst 5:1877–1888, doi: 10.1039/b906391a
20. Bairoch A, Apweiler R (1997) The SWISS-PROT protein sequence data bank and its supplement TrEMBL. Nucleic Acids Res 25(1):31–36
21. Innis CA, Shi J, Blundell TL (2000) Evolutionary trace analysis of TGF-beta and related growth factors: implications for site-directed mutagenesis. Protein Eng 13(12):839–847
22. Waterhouse AM, Procter JB, Martin DM, Clamp M, Barton GJ (2009) Jalview Version 2—a multiple sequence alignment editor and analysis workbench. Bioinformatics 25(9):1189–1191
23. Lichtarge O, Bourne HR, Cohen FE (1996) An evolutionary trace method defines binding surfaces common to protein families. J Mol Biol 257(2):342–358. doi:10.1006/jmbi.1996.0167
24. Lin F, Wang R (2009) Molecular modeling of the three-dimensional structure of GLP-1R and its interactions with several agonists. J Mol Model 15(1):53–65. doi:10.1007/s00894-008-0372-2